Available online at www.sciencedirect.com

ScienceDirect

Physics Procedia 3 (2010) 1231–1236

Physics Procedia

www.elsevier.com/locate/procedia

14th International Conference on Narrow Gap Semiconductors and Systems

Oscillatory quantum interference effects in narrow-gap semiconductor heterostructures

R.B. Lillianfeld[1]*, R.L. Kallaher[1], J.J. Heremans[1]†, Hong Chen[2], N. Goel[3], S.J. Chung[3], M.B. Santos[3], W. Van Roy[4], G. Borghs[4]

[1]*Department of Physics, Virginia Tech, Blacksburg, VA 24061, USA*
[2]*Department of Physics, University of North Florida, Jacksonville, FL 32224, USA*
[3]*Homer L. Dodge Department of Physics and Astronomy, University of Oklahoma, Norman, OK 73019, USA*
[4]*IMEC, Leuven, Belgium*

Abstract

We investigate quantum interference phenomena in narrow bandgap semiconductors under strong spin-orbit interaction, by measuring the magnetoresistance across mesoscopic closed-path structures fabricated in two-dimensional electron systems. We discuss our results in terms of four quantum interference effects brought about by geometric phases acquired by the electron wave functions: the Aharonov-Bohm phase, the Altshuler-Aronov-Spivak effect, the Berry's phase due to the evolution of the spin degree of freedom, and the Aharonov-Casher phase.

Keywords: Aharonov-Bohm effect, quantum interference, spin orbit interaction

1. INTRODUCTION

Quantum interference effects are a hallmark of mesoscopic physics [1]. The structure of periodic oscillations in the magnetoresistance (MR) of closed-loop structures yields evidence of geometric phases acquired by the electron wave function [2-8]. We examine quantum interference in devices fabricated in InAs/AlGaSb and InSb/InAlSb two-dimensional electron systems (2DESs); and find behavior characteristic of several different quantum-mechanical phases: interference brought about by the Aharonov-Bohm (AB) phase [9, 10] arising from magnetic flux threading mesoscopic rings, as well as Altshuler-Aronov-Spivak (AAS) interference [10] arising from AB phase differences between exact time-reversed paths; a Berry's phase [2-8] due to the spin degree of freedom, and

*rblilli@vt.edu
† heremans@vt.edu

doi:10.1016/j.phpro.2010.01.168

the electromagnetic dual of the AB phase – the Aharonov-Casher (AC) phase [8, 11]. Studying these phases in narrow-gap semiconductors has been used to gain information on decoherence mechanisms and spin-orbit interaction (SOI) in 2DESs [12, 13].

2. EXPERIMENT

2.1 InAs / AlGaSb

Ring arrays were fabricated using electron beam lithography and inductively coupled plasma reactive ion etching (ICP-RIE) on Hall bars that were defined on an InAs/AlGaSb heterostructure by photolithography and wet etching. The MBE grown InAs/AlGaSb heterostructure has a 15 nm InAs well under a 20 nm $Al_{0.2}Ga_{0.8}Sb$ cap layer. The heterostructure does not contain intentional doping layers [14]. Mobilities as high as $\mu = 36.5$ m^2/V s were measured at a temperature $T = 0.4$ K in unpatterned regions. Carrier density at $T < 10$ K is $N_s = 8.5 \times 10^{15}$ m^{-2}. The ring arrays consist of seven columns of seven rings each, connected serially (Fig. 2 inset). The rings have an average radius of 350 nm and a lithographic arm width of 130 nm. MR measurements over the ring arrays were obtained at $T = 0.4$ K by sweeping a magnetic field B perpendicular to the 2DES, up to $B = 9$ T. Low-field MR ($B <$ 200 mT) was obtained from 0.4 K < T < 10 K in order to study the T-dependence of the quantum oscillations. Figures 1 and 2 contain examples of MR measurements.

2.2 InSb / InAlSb

A periodic square network, illustrated in Fig. 3, was fabricated on an InSb/InAlSb heterostructure by electron beam lithography and wet etching. The square network contains 1250 cells, arranged in parallel necklaces of cells repeating at 1.2 μm intervals and separated by 1.4 μm. The MBE grown InSb/InAlSb heterostructure has a 25 nm InSb quantum well, flanked by $In_{0.85}Al_{0.15}Sb$ barriers. The well resides at 163 nm below the surface and electrons are provided to the well by two δ–doped layers, at 40 nm above and 40 nm below the well. Surface states are passivated by a third δ–doped layer located 23 nm below the surface. At $T = 0.4$ K, $\mu = 8.0$ m^2/Vs and $N_s = 6 \times 10^{15}$ m^{-2} were measured in unpatterned regions. The sample is front-gated with a 1.3 μm polyimide dielectric ($\varepsilon = 3.4$) and a Cr/Au gate electrode. Low-field MR measurements were obtained at front-gate voltages, V_g, ranging from -18 V ≤ V_g ≤ 10 V at $T = 0.4$ K, and at V_g ranging from -10 V ≤ V_g ≤ 8 V at $T = 4$ K.

3. RESULTS

3.1 Simultaneous Observation of AB and AAS Oscillations in InAs / AlGaSb

When two possible paths of an electron enclose magnetic flux, an observable interference effect occurs due to the phase difference, $\Delta\phi_{AB}$, between the two paths [9]:

$$\Delta\phi_{AB} = \frac{1}{\hbar}\oint q\,(\boldsymbol{A}\cdot\boldsymbol{dl}) = \frac{e\Phi}{\hbar} = 2\pi\frac{\Phi}{\Phi_0} \tag{1}$$

Here e represents the charge of the electron, the magnetic flux enclosed by the paths is denoted Φ, and $\Phi_0 = h/e$. The interference is known as the Aharonov-Bohm (AB) effect [9]. Random scattering-induced phase differences between paths about a loop are expected to average out AB interference in measurements involving many loops [10]. Nonetheless, there is a special subset of trajectories, pairs that are exact time reversals of each other, which encounter the same scattering events, and thus show no scattering-dependent phase difference [1]. The interference between these pairs leads to the Altshuler-Aronov-Spivak (AAS) effect, expected to be the dominant contribution to MR oscillations in large arrays [10]. Because each time-reversed path travels around the entire loop, the total flux enclosed by AAS trajectories is twice that of AB trajectories, causing AAS interference with a fundamental period of $\Phi_0/2 = h/2e$. The pronounced minimum in MR at $B = 0$ is characteristic of both AAS and antilocalization in systems with strong SOI [7, 15], and results from destructive quantum interference of spin ½ carriers rotated over a relative 2π angle [15]. In AB interference, however, the random phase differences between paths do not result in an obligatory minimum at $B = 0$. Indeed the presence of a maximum or minimum at $B = 0$ in AB oscillations appears to be dependent on impurity configuration, as we have observed both maxima and minima after thermal cycling of

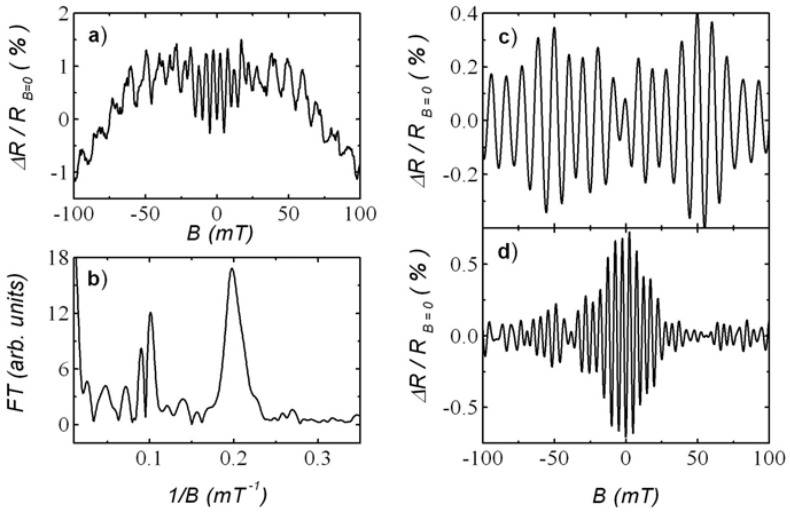

Figure 1- a) MR of rings in the InAs / AlGaSb 2DES at $T = 0.4$ K. Higher-frequency oscillations at low B are AAS ($h/2e$) oscillations; AB (h/e) oscillations dominate at $|B| > 50$ mT. b) FT of data from (a). The FT data range (-100 mT < B < 100 mT) includes the AAS signal and 20 periods of the AB signal. The magnitude of the splitting in the AB peak is 0.011mT^{-1}. c) Digital filtering isolates the h/e and (d) $h/2e$ components of the oscillations represented in (a).

the sample. As magnetic fields break time reversal symmetry, AAS oscillations decay with increasing B, owing to the decrease in number of suitable time reversed pairs, which distinguishes AAS interference from the higher harmonics of AB interference that do not require time-reversal symmetry.

The data in Figs. 1 and 2 show a clear periodic modulation of the ring array MR. At higher fields ($B > 50$ mT) the modulation in MR is dominated by oscillations with a period of 10 mT, corresponding to an Aharonov-Bohm flux through individual rings of h/e, whereas at very low B ($B < 50$ mT) the MR oscillates with a period of 5.0 mT, corresponding to a flux through the rings of $h/2e$. After subtracting the low-frequency MR background due to localization, a Fourier transformation of the MR (FT) confirms the periodicity of the oscillations (Fig. 1). Additionally, the FT allows us to examine the different components of the MR oscillations independently (Fig. 1), maintains phase information, and enables us to quantify oscillation amplitudes.

We quantify relative amplitudes of h/e and $h/2e$ oscillations by performing the FT and integrating over frequency ranges that correspond to the lithographic inner and outer radii of the rings. The relatively high amplitude of $h/2e$ oscillations compared to h/e oscillations for low-field FTs, coupled with the lower amplitude of $h/2e$ oscillations compared to h/e oscillations for high-field FTs over identical field ranges, indicates that main contribution to $h/2e$ oscillations is indeed AAS interference. Thus, while digital filtering reveals the presence of $h/2e$ oscillations that persist to high B, characteristic of second harmonic AB interference, it is clear that the strong $h/2e$ contribution at low B that decays rapidly with increasing B results indeed from AAS interference.

It is notable that we observe both strong AB oscillations and strong AAS oscillations in our ring arrays. While AB and AAS oscillations have been observed simultaneously in single rings and large arrays [16, 17], it is unusual to observe both with such closely comparable amplitudes. The simultaneous observation of the two interference phenomena in an array has been interpreted as evidence that the device dimensions are comparable to the phase coherence length, L_ϕ [17], correlating the behavior of adjacent rings.

3.2 Temperature dependence of AB and AAS oscillations in InAs / AlGaSb

The amplitude of the AB oscillations (A_{AB}) is widely assumed to relate to L_ϕ by $A_{AB} \sim \exp(-L/L_\phi)$, where L is the path-length [16]. We therefore examine the dependence on T of the oscillation amplitudes in order to gain

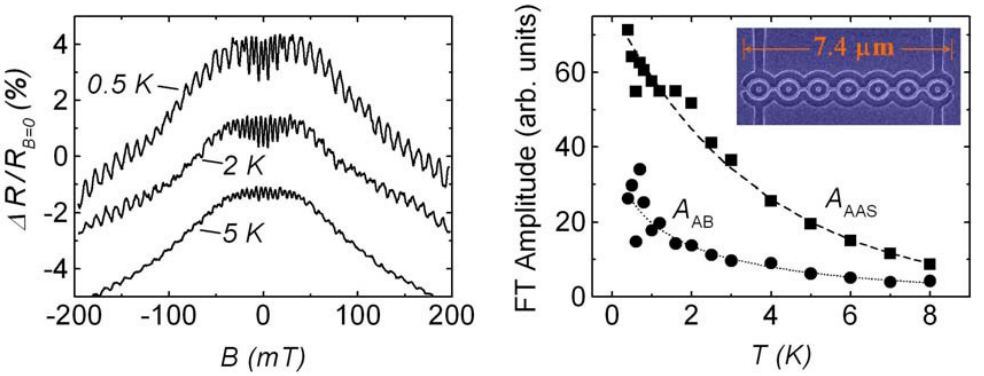

Figure 2- (left) MR of rings at T = 0.5 K, 2 K, and 5 K. The curves are offset for clarity. (right) T-dependence of AAS and AB oscillation amplitudes. The fits are shown for both $A_{AAS} = 76.7 \exp[-(T / 3.71)]$ (dashed line) and $A_{AB} = 49.2 \exp[-(T / 1.20)^{1/2}]$. (right-inset) SEM micrograph of the ring pattern.

information on the dependence of L_ϕ on T. Figure 2 shows evolution over T of A_{AB} and the amplitude of the AAS oscillations, A_{AAS}, obtained from FTs for -100 mT < B < 100 mT. Both the A_{AB} and A_{AAS} decay rapidly as T increases from 0.4 K. This is consistent with the expected exponential dependence of oscillation amplitude on L_ϕ.

Assuming the dependence $(1/L_\phi) \sim T^P$, where $P>0$, we quantify the T-dependence of $A_{AB(AAS)}$ by fitting the data presented in Fig. 2 to $A_{AB(AAS)}=C\exp(-(T/T_0)^P)$, where C, P, and T_0 are fitting parameters. From these fits we find $1/3 \leq P_{AB} \leq 1/2$, and $P_{AAS} = 1$. The weaker T-dependence for A_{AB} as compared to A_{AAS} reflects differences in the physical mechanisms underlying the interference phenomena. From the extracted range of P_{AB} we conclude that L_ϕ follows a T-dependence which is consistent with the Nyquist electron-electron dephasing mechanism, where for 2D systems $L_\phi^2 \equiv D\tau_\phi \sim T^{-1}$ (D being the diffusion constant) and $L_\phi^2 \sim T^{-2/3}$ for quasi 1D systems [18].

3.3 Peak splitting in Fourier transforms of InAs / AlGaSb MR

A prominent feature in the FT of the InAs / AlGaSb rings at all T is a strong splitting in the AB peak (Fig. 1). Splitting has been observed in the FTs of single rings [2, 4, 7], ring arrays and antidot arrays [6], and FTs averaged over several impurity configurations [19], and in several different material systems. While it is understood that some structure in the FT can arise from the finite conducting width of the rings [1], the splitting has also been explained as a possible observation of a (geometric) Berry's phase induced by SOI [2-7].

When a quantum-mechanical object's parameter space undergoes a cyclic evolution, the wave function will acquire a phase independent of the dynamic nature of the evolution. This phase is known as a geometric phase. When the evolution occurs adiabatically it is referred to as a Berry's phase. SOI can be viewed as producing an effective intrinsic magnetic field [7], $\mathbf{B_{int}}$, which is perpendicular to both the particle's momentum and the electric field responsible for the SOI [20]. For a 2DES with strong Rashba SOI, $\mathbf{B_{int}}$ lies in the plane of the 2DES [20], with $|\mathbf{B_{int}}| = 2\alpha k_F / g\mu_B$, where α parameterizes the strength of the Rashba SOI, k_F is the Fermi wavevector, g is the gyromagnetic ratio, and μ_B represents the Bohr magneton. The total magnetic field the particle experiences is the vector sum of the intrinsic and the external fields, $\mathbf{B_{total}} = \mathbf{B_{ext}} + \mathbf{B_{int}}$ [7]. A particle traveling about a loop, therefore, experiences a cyclic change in the direction of $\mathbf{B_{total}}$ and acquires a geometric phase [2-7].

It has been predicted [4-7] that in the adiabatic limit a SOI induced Berry's phase should be manifested as a splitting in h/e and $h/2e$ peaks in the FT, and consequentially as a beating in the MR itself, as spin up and spin down will add a phase of opposite sign to their AB phase [7]. The magnitude of the spitting of the FT peaks has been predicted to relate to $\mathbf{B_{int}}$ by [5]:

$$\frac{1}{B_{\text{int}}} = \frac{1}{2B_{h/2e\,\text{sp}}} = \frac{1}{B_{h/e\,\text{sp}}} \qquad (2)$$

where $1/B_{h/e\ (h/2e)\ sp}$ is the splitting in the *h/(2)e* FT peak. Beating in the AB component of the MR is evident in the raw data and highlighted by digital filtering (Fig. 1). The observed beat frequency of $(90\ \text{mT})^{-1}$ in MR matches the splitting in the AB FT peak, and does not vary significantly with T. This implies $B_{int} = 90$ mT and corresponds to $\alpha = 1.8\text{x}10^{-13}$ eV m. Shubnikov-de Haas measurements on samples from the same wafer yield $B_{int} = 3.9$ T and $\alpha = 7.8\text{x}10^{-12}$ eV m. This discrepancy was also observed in Ref. 7. Similarly to Ref. 7 this discrepancy could arise because our system lies in the crossover between the diffusive and ballistic regimes, and our measurements are not performed in B sufficiently high to ensure adiabaticity.

3.4 Gate-Voltage Dependence of MR in InSb / InAlSb

Figure 3 contains MR oscillations observed at $T = 0.4$ K under variable front-gate voltage V_g in the InSb periodic network. Oscillations with periodicity of 4.0 mT are clearly visible. The periodicity results from *h/2e* oscillations and corresponds to an orbit encompassing an effective area of 0.52 μm^2. The area corresponds to a non-circular, slightly elongated, average orbit fitting in one cell with semi-axes of ~ 350 nm and ~ 470 nm respectively (Fig. 3). V_g from -18 V to 10 V could be applied without gate leakage becoming problematic, with the range corresponding to ~ 15% change in N_s. Larger variations in N_s were precluded due to electron ($V_g > 0$) or hole ($V_g < 0$) accumulation in the heterostructure's cap layer. Figure 3 shows a contour plot of the MR vs V_g and B. In general, the oscillation amplitude increases at more negative V_g, due to the concomitant decrease in N_s. A decrease in N_s leads to an increase in the depletion width, and hence a decrease in conducting width of the channel. The trajectories gain a better definition, leading to more vigorous oscillations [21]. Further, a broadening of the MR background is observed at more positive V_g. The broadening can be ascribed to a decrease in spin coherence length as N_s increases in response to V_g.

Riding on the general trends described above, a quasi-periodic modulation of the oscillation amplitude with variable V_g is discernable (for instance in the amplitude of the second oscillation, with maxima indicated by white lines on the plot), with a tentative periodicity in V_g of ~10 V. The monotonic variation of N_s with V_g precludes an explanation in terms of conducting widths and spin coherence lengths. Hence, and although more detailed measurements are presently impeded by the difficulty in gating the narrow-gap InSb heterostructures over a wider range of N_s, we ascribe the modulation to the time-reversal Aharonov-Casher effect [8]. The time-reversal Aharonov-Casher effect can be regarded as an electromagnetic dual to the AAS effect [11], and results from spin interference under an applied electric field which modulates the spin-orbit interaction in the heterostructure. Scaling

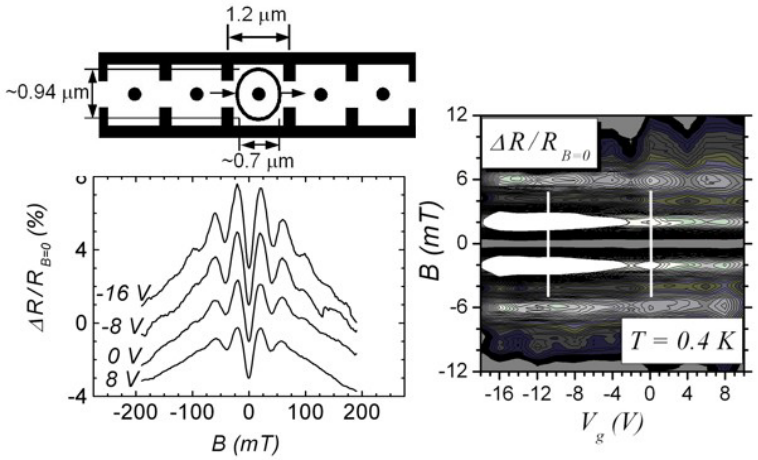

Figure 3- (bottom-left) Low field MR of the InSb / InAlSb square network at $T = 0.4$ K for various values of the top-gate voltage (V_g). Curves are offset for clarity. (right) Contour plot of the MR as a function of V_g, with lines indicating local amplitude maxima. (top-left) Schematic of the network.

with the respective strengths of the Rashba spin-orbit interaction and gate dielectric thicknesses, the periodicity in V_g is in accordance with a previous observation of the effect [8] on InGaAs quantum wells. In these measurements, using a 80 nm gate dielectric, a periodicity of ~ 1 V was observed on a heterostructure with Rashba coefficient $\alpha \approx 5x10^{-12}$ eV m. Since our measurements use a dielectric ~ 16 times thicker, and since α in InSb quantum wells can reach $1x10^{-11}$ eV m [22], we expect a periodicity ~ 8 V, in agreement with the observed value of ~10 V. We note however that the present gating constraints limit the conclusions we can draw from the observed modulation in V_g.

4. CONCLUSION

In summary, we have observed quantum interference effects in the MR of mesoscopic closed path structures fabricated from narrow-gap 2DESs. Strong AB and AAS oscillations are observed in ring arrays fabricated from an InAs/AlGaSb 2DES. We find separate *T*-dependences for AB and AAS oscillation amplitudes with the AB oscillation amplitude indicating that the Nyquist electron-electron mechanism governs phase decoherence. Analyzing the observed 90 mT splitting of the AB peak in terms of a SOI induced Berry's phase leads to a Rashba parameter $\alpha = 1.8x10^{-13}$ eV m, which is ~40 times smaller than α determined from beating in Shubnikov de Haas oscillations. Separately, we present the gate voltage dependence of AAS oscillations in a periodic square network fabricated from an InSb/InAlSb 2DES. We note a quasi-periodic modulation in the oscillation amplitude as a function of gate voltage with a periodicity that is consistent with the time-reversal Aharonov-Casher effect. The authors acknowledge support from grants DOE DE-FG02-08ER46532 and NSF DMR-0520550.

REFERENCES

1. E. Akkermans and G. Montambaux, *Mesoscopic Physics of Electrons and Photons* (Cambridge University Press, Cambridge, 2007).
2. J.B. Yau *et al.*, Phys. Rev. Lett. **88**, 146801 (2002).
3. D. Loss *et al.*, Phys. Rev. B **59**, 13328 (1999).
4. A.F. Morpurgo *et al.*, Phys. Rev. Lett. **80**, 1050 (1998).
5. H.A. Engel and D. Loss, Phys. Rev. B **62**, 10238 (2000).
6. N. Kang *et al.*, J. Phys. Soc. Jpn. **76**, 83704 (2007).
7. B. Grbić *et al.*, Phys. Rev. Lett. **99**, 176803 (2007).
8. T. Bergsten *et al.*, Phys. Rev. Lett. **97**, 196803 (2006).
9. Y. Aharonov and D. Bohm, The Physical Review **115**, 485 (1959).
10. S. Washburn and R. Webb, Advances in Physics **35**, 375 (1986).
11. Y. Aharonov and A. Casher, Phys. Rev. Lett. **53**, 319 (1984). H. Mathur and A.D. Stone, Phys. Rev. Lett. **68**, 2964 (1992).
12. M. Ferrier *et al.*, Phys. Rev. Lett. **100**, 146802 (2008).
13. A.E. Hansen *et al.*, Phys. Rev. B **64**, 045327 (2001).
14. C. Nguyen *et al.*, Appl. Phys. Lett. **60**, 1854 (1992).
15. G. Bergmann, Phys. Rep. **107**, 1 (1984).
16. C.P. Umbach *et al.*, Phys. Rev. Lett. **56**, 386 (1986).
17. F. Schopfer *et al*., Phys. Rev. Lett. **98**, 026807 (2007).
18. J.J. Lin and J.P. Bird, J. Phys: Condens. Matter **14**, R501 (2002), and refs. therein.
19. F.E. Meijer *et al.*, Phys. Rev. B **69**, 035308 (2004).
20. R. Winkler, *Spin Orbit Coupling Effects in Two Dimensional Electron and Hole Systems*, (Springer-Verlag, New York, 2003).
21. B. Douçot and R. Rammal, Phys. Rev. Lett. **55**, 1148 (1985).
22. H. Chen *et al.*, Appl. Phys. Lett. **86**, 032113 (2005).